

## Novel Electronic States of Topological Crystalline Insulators Revealed by ARPES

Topological insulators are a novel quantum state of matter where unusual gapless metallic states protected by time-reversal symmetry appear within the bulk band gap. A recent theory predicted another type of topological material called topological crystalline insulator (TCI), where the surface states are protected by mirror symmetry of the crystal. We have performed angle-resolved photoemission spectroscopy of narrow-gap IV-VI semiconductor  $\text{Pb}_{1-x}\text{Sn}_x\text{Te}$  as a function of Pb content  $x$  and found clear evidence for the topological phase transition from TCI to trivial insulator. The present result establishes the essential role of the crystal mirror symmetry in realization of the TCI phase.

The discovery of topological insulators (TIs) triggered the search for new types of topological materials protected by various symmetries, and a recent theory predicted the existence of *topological crystalline insulators* (TCIs) in which metallic surface states are protected by mirror symmetry of the crystal structure [1, 2]. Such a TCI phase has been experimentally verified by angle-resolved photoemission spectroscopy (ARPES) experiments for narrow-gap IV-VI semiconductor SnTe [3, 4] and related compounds [5]. In those materials, the topological surface states on the (001) surface consist of Dirac cones located at momenta slightly away from the time-reversal-invariant momentum (TRIM)  $\bar{X}$  point in the (110) mirror plane of the crystal [Fig. 1(a)], producing a characteristic double Dirac-cone band dispersion. This is distinct from the three-dimensional TIs whose surface states are characterized by an odd number of Dirac cones. In contrast to the double Dirac-cone signature observed in the TCI phase, the ARPES measurements for isostructural PbTe [3] revealed the absence of any surface states, which strongly suggests a trivial-to-non-trivial topological quantum phase transition in the solid-solution system  $\text{Pb}_{1-x}\text{Sn}_x\text{Te}$ . However, it is still unclear how the surface and bulk electronic states evolve as a function of Sn composition  $x$ , which would be useful for attaining a practical understanding of TCIs.

To elucidate the electronic states of  $\text{Pb}_{1-x}\text{Sn}_x\text{Te}$ , we have performed high-resolution ARPES experiments at BL-28A and Tohoku University [6, 7].

Figure 1(b) shows the Fermi-surface mapping around the  $\bar{X}$  point of the surface Brillouin zone (BZ) for  $\text{Pb}_{1-x}\text{Sn}_x\text{Te}$  with four representative Sn compositions  $x$  including both end members SnTe ( $x = 1.0$ ) and PbTe ( $x = 0.0$ ). At  $x = 1.0$ , we immediately notice a dumbbell-shaped intensity pattern elongated along the  $\bar{\Gamma}\bar{X}$  direction ( $k_x$  direction) with its intensity maxima located away from the  $\bar{X}$  point. This feature arises from the double Dirac-cone surface state [3] whose Dirac points are located at each intensity maxima, as one can see from the near- $E_F$  band dispersion along the  $\bar{\Gamma}\bar{X}$  cut in Fig. 1(c) showing the band maxima on both sides of the  $\bar{X}$  point. The M-shaped dispersion and the dumbbell-shaped Fermi surface are also observed for  $x = 0.5$ , which sig-

nifies that the system still belongs to the TCI phase, although the intensity distribution around  $E_F$  appears to be weaker and broader than that for  $x = 1.0$ . At  $x = 0.3$ , the observed ARPES intensity looks different, and neither the dumbbell-shaped Fermi surface nor the M-shaped dispersion are clearly resolved. Nevertheless, we are still able to trace the surface-band dispersion by taking second derivatives of the intensity and, as shown in Fig. 1(d), the M-shaped dispersion is still discernible. In contrast, the spectral feature for  $x = 0.0$  looks substantially different. The near- $E_F$  intensity is strongly suppressed and no Dirac-cone surface band is observed, reflecting the topologically trivial (ordinary) nature of PbTe [3]. A more systematic ARPES experiment for various  $x$  and photon energies further revealed that the topological phase transition takes place at  $x \sim 0.25$  [6].

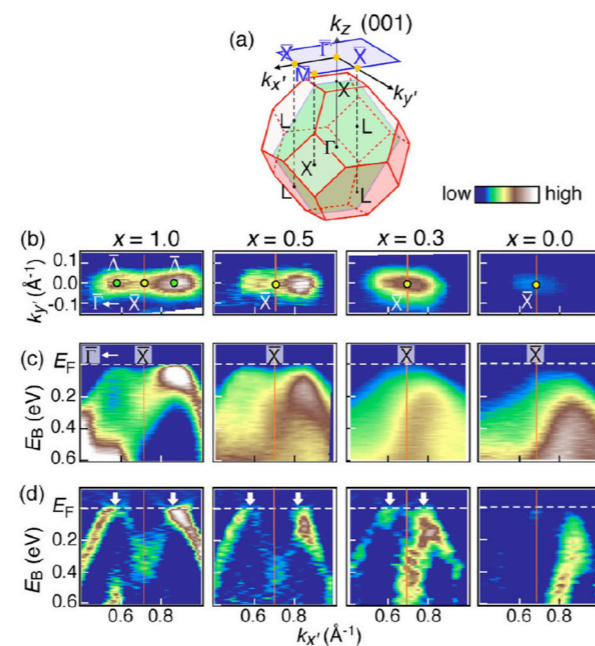


Figure 1: (a) Bulk Brillouin zone (BZ) and corresponding surface BZ of  $\text{Pb}_{1-x}\text{Sn}_x\text{Te}$ . The (110) mirror plane is indicated by the green shaded area. (b) ARPES intensity at  $E_F$  around the  $\bar{X}$  point for various  $x$  values plotted as a function of in-plane wave vector at  $T = 30$  K [6]. (c) Corresponding near- $E_F$  ARPES intensity along the  $\bar{\Gamma}\bar{X}$  cut plotted as a function of  $k_x$  and binding energy  $E_B$ . (d) Band dispersions derived from the second derivatives of the momentum distribution curves (MDCs) along the  $\bar{\Gamma}\bar{X}$  cut. The  $k$  location of the Dirac point is indicated by white arrows in (d).

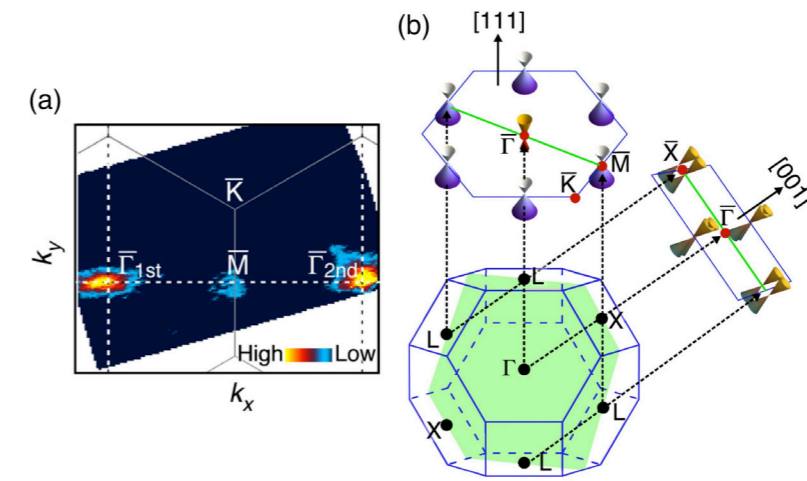


Figure 2: (a) ARPES intensity mapping at  $E_F$  of SnTe on the (111) surface plotted as a function of in-plane wave vector [7]. (b) Schematic picture of the Dirac-cone surface state on two different surface planes of (001) and (111). The green shaded area and green line represent the (110) mirror plane and the mirror-symmetric line on the surface BZ, respectively.

The most important feature is the evolution of the surface state in the TCI phase. In particular, as seen in Fig. 1(d), the  $k$  position of the Dirac point in the BZ systematically moves toward the  $\bar{X}$  point with decreasing  $x$  (see white arrows). Such a degree of freedom is obviously a unique feature of the mirror-symmetry protected TCIs, in contrast to the TIs where the Dirac point is bound to the TRIM. Intuitively, the double Dirac-cone structure in TCIs is a result of the hybridization of two Dirac cones, because, on the (001) surface, two L points (which are each responsible for a surface Dirac cone due to the band inversion at L) are projected onto the same  $\bar{X}$  point; therefore, the separation of the two Dirac cones can be taken as a measure of this hybridization. Our finding is of crucial importance for establishing a better understanding of the physical mechanism to create the peculiar double Dirac-cone structure in TCIs. Also, the mobile Dirac cone is particularly useful in applications requiring Fermi-surface matching with other materials, like spin injection.

To see whether or not the Dirac-cone band dispersion is a unique feature of the (001) surface, we also performed an ARPES measurement on the (111) surface. As shown in Fig. 2(a), one can immediately recognize the bright intensity centered at the first and second  $\bar{\Gamma}$  points as well as the relatively weak intensity at the  $\bar{M}$  point of the hexagonal surface BZ. This intensity pattern originates from the Dirac-cone surface states centered at the  $\bar{\Gamma}$  and  $\bar{M}$  points, respectively [7]. Figure 2(b) compares the observed Dirac-cone surface states between the (001) and (111) surfaces. The surface states for the (001) surface consist of a double-Dirac-cone structure. On the other hand, for the (111) surface, always a single L point is projected onto either the  $\bar{\Gamma}$  or  $\bar{M}$  point to

produce a single Dirac cone centered at those TRIMs, and no band hybridization takes place. As a result, the Dirac point coincides with the  $\bar{\Gamma}$  and  $\bar{M}$  points. The present ARPES result thus allows for the first time a direct comparison of topological surface states on different crystal faces of a topological material, and establishes the essential role of the crystal mirror symmetry in realization of the TCI phase.

### REFERENCES

- [1] L. Fu, *Phys. Rev. Lett.* **106**, 106802 (2011).
- [2] T.H. Hsieh, H. Lin, J. Liu, W. Duan, A. Bansil and L. Fu, *Nature Commun.* **3**, 982 (2012).
- [3] Y. Tanaka, Z. Ren, T. Sato, K. Nakayama, S. Souma, T. Takahashi, K. Segawa and Y. Ando, *Nature Phys.* **8**, 800 (2012).
- [4] S.-Y. Xu, C. Liu, N. Alidoust, M. Neupane, D. Qian, I. Belopolski, J.D. Denlinger, Y.J. Wang, H. Lin, L.A. Wray, G. Landolt, B. Slomski, J.H. Dil, A. Marcinkova, E. Morosan, Q. Gibson, R. Sankar, F.C. Chou, R.J. Cava and A. Bansil, *Nature Commun.* **3**, 1192 (2012).
- [5] P. Dziawa, B.J. Kowalski, K. Dybko, R. Buczko, A. Szczerbakow, M. Szot, E. Łusakowska, T. Balasubramanian, B.M. Wojek, M.H. Berntsen, O. Tjernberg and T. Story, *Nature Mater.* **11**, 1023 (2012).
- [6] Y. Tanaka, T. Sato, K. Nakayama, S. Souma, T. Takahashi, Z. Ren, M. Novak, K. Segawa and Y. Ando, *Phys. Rev. B* **87**, 155105 (2013).
- [7] Y. Tanaka, T. Shoman, K. Nakayama, S. Souma, T. Sato, T. Takahashi, M. Novak, K. Segawa and Y. Ando, *Phys. Rev. B* **88**, 235126 (2013).

### BEAMLIN

BL-28A

T. Sato<sup>1</sup>, Y. Tanaka<sup>1</sup>, T. Shoman<sup>1</sup>, K. Nakayama<sup>1</sup>, S. Souma<sup>1</sup>, T. Takahashi<sup>1</sup>, M. Novak<sup>2</sup>, K. Segawa<sup>2</sup> and Y. Ando<sup>2</sup> (<sup>1</sup>Tohoku Univ., <sup>2</sup>Osaka Univ.)